

# **Optimal alignment of mirror based pentaprisms for scanning deflectometric devices**

Samuel K. Barber <sup>a†</sup>, Ralf D. Geckeler <sup>b</sup>, Valeriy V. Yashchuk<sup>\*a</sup>, Mikhail V. Gubarev <sup>c</sup>,  
Jana Buchheim <sup>d</sup>, Frank Siewert <sup>d</sup>, and Thomas Zeschke<sup>d</sup>

<sup>a</sup>Lawrence Berkeley National Laboratory, One Cyclotron Road, Berkeley, CA 94720, USA

<sup>b</sup>Physikalische-Technische Bundesanstalt, Bundesallee 100, 38116 Braunschweig, Germany

<sup>c</sup>NASA Marshall Space Flight Center (MSFC), Huntsville, AL 35812, USA

<sup>d</sup>Helmholtz Zentrum Berlin für Materialien und Energie, Elektronenspeicherring BESSY-II,  
Albert-Einstein-Str. 15, 12489 Berlin, Germany

\*Corresponding author: [VYashchuk@lbl.gov](mailto:VYashchuk@lbl.gov)

† Currently at University of California, Los Angeles

## ABSTRACT

In the recent work [*Proc. of SPIE* **7801**, 7801-2/1-12 (2010), *Opt. Eng.* **50**(5) (2011), in press], we have reported on improvement of the Developmental Long Trace Profiler (DLTP), a slope measuring profiler available at the Advanced Light Source Optical Metrology Laboratory, achieved by replacing the bulk pentaprism with a mirror based pentaprism (MBPP). An original experimental procedure for optimal mutual alignment of the MBPP mirrors has been suggested and verified with numerical ray tracing simulations. It has been experimentally shown that the optimally aligned MBPP allows the elimination of systematic errors introduced by inhomogeneity of the optical material and fabrication imperfections of the bulk pentaprism. In the present article, we provide the analytical derivation and verification of easily executed optimal alignment algorithms for two different designs of mirror based pentaprisms. We also provide an analytical description for the mechanism for reduction of the systematic errors introduced by a typical high quality bulk pentaprism. It is also shown that residual misalignments of an MBPP introduce entirely negligible systematic errors in surface slope measurements with scanning deflectometric devices.

**Keywords:** optical metrology, surface slope metrology, surface profilometer, long trace profiler, LTP, developmental LTP, pentaprism, mirror based pentaprism, alignment, deflectometry

## 1. INTRODUCTION

Starting from the canonical and often repeated tenet that the quality of x-ray and EUV optics must improve to keep pace with the ever evolving next generation light sources, we acknowledge that error reduction in metrological instruments and techniques is vital. From SEM and TEM on the small scale to scanning deflectometric devices at the large scale, there will always be room for improvement.

In the realm of flat and slightly curved synchrotron optics, the primary factors limiting the overall beamline performance tend to be the figure error and RMS slope variation. At present, and for the foreseeable future, optical scanning deflectometric devices provide the highest quality metrology for these types of optics. Currently, requirements for these optics<sup>1,2</sup> are pushing the limits of the absolute accuracy of even the best optical scanning deflectometric devices, i.e. the the Nanometer Optical Component Measuring Machine (NOM) at Helmholtz Zentrum Berlin (HZB)/BESSY-II (Germany)<sup>3-6</sup> and the Extended Shear Angle Difference (ESAD) instrument at PTB (Germany).<sup>7-9</sup>

With this in mind we undertook a systematic review of the fundamental components involved in a typical scanning deflectometric device and identified the scanning pentaprism as a component potentially limiting overall performance, which can easily be improved upon. By replacing traditional bulk material pentaprisms with a mirror based alternative, the two refracting interfaces and complexities due to potentially inhomogeneous material are eliminated. In addition, a mirror based pentaprism (MBPP) allows for far greater quality control when selecting the reflecting components. In any pentaprism system, the combination of the topography of each of the reflecting (and refracting) faces leads to an effective curvature, which imbues the pentaprism with a focusing/defocusing quality. Using a mirror based pentaprism allows one to

suppress this spurious focusing effect through the selection of high quality mirrors and optimizing their relative orientation.

In recent work,<sup>10</sup> we have reported on improvement of the Developmental Long Trace Profiler (DLTP),<sup>11</sup> a low budget slope measuring profiler available at the Advanced Light Source Optical Metrology Laboratory (OML), achieved by replacing the bulk pentaprism with an MBPP. An original experimental procedure for optimal mutual alignment of the pentaprism mirrors has been suggested and verified with numerical ray tracing simulations. It has been experimentally shown that the optimally aligned MBPP allows for elimination of systematic errors introduced by inhomogeneity of the optical material and fabrication imperfections of the bulk pentaprism and to significantly improve the reliability of the DLTP measurements. Measurements of flat and slightly curved optics made with the upgraded DLTP have shown that the overall absolute accuracy is very close to 50 nrad, which is the limit set by the specified repeatability of the autocollimator in use.

In this paper we analytically demonstrate how the performance of a typical deflectometric scanning device can be improved by switching from a typical bulk pentaprism to an optimized MBPP. We address the concern of alignment of the MBPP by including two optimal alignment procedures, which are derived from an analytic consideration of the problem. The two procedures are suitable for different MBPP designs, which have different advantages. Furthermore, through our analytic derivations we show that residual misalignments of the MBPP contribute a negligible systematic error to optical scanning deflectometric measurements. Our analytical approach to the problem of optimal alignment of mirrors of an MBPP is an extension of the method for optimal alignment of a bulk pentaprism of a scanning deflectometric device presented in Ref.<sup>12</sup>

## 2. DEFLECTOMETER'S SYSTEMATIC ERROR RELATED TO PENTAPRISM

In the deflectometric device under consideration, a scanning pentaprism is used to optically connect the surface under test (SUT) and an optical slope measuring sensor (e.g., autocollimator, pencil beam interferometer, etc.). A scanning pentaprism arrangement effectively solves the problem of measurement error due to wobbling of the translated carriage.<sup>13</sup>

However, there are three primary concerns with using a traditional bulk pentaprism. The first is related to the requirements for precise mutual alignment of the pentaprism, optical sensor, and translation system.<sup>10,12</sup> Basically, this problem does not depend on type of pentaprism; however, as we show below, it can be more easily addressed with the use of an MBPP.

The second concern is related to the bulk material itself. As the tilt angle of the surface under test varies, so too does the optical path through the bulk material. Thus, any inhomogeneity in the material will introduce an error in the measurements. By construction, an MBPP does not suffer from any such complexities.

The third concern with a bulk pentaprism is the figure errors of the reflecting and refracting surfaces. In the first approximation, the figure errors can be modeled with as an effective curvature. Although an MBPP will have an effective curvature as well, the control of such an effect is significantly greater as suitable mirrors can be hand selected and oriented.<sup>10</sup> The result of such an effective curvature is the contribution of a systematic error to measurements, which primarily manifests itself when measuring curved optics.

To understand consequences of the effective curvature, we model the pentaprism as a curved mirror oriented such that a ray traveling along the longitudinal axis of the autocollimator is reflected by exactly 90 degrees towards the surface under test, Fig. 1. In this case, if the incoming ray is not incident perfectly normal on the SUT, then the ray reflected back will be

incident on a different point of the curved mirror. Conceptually, there is a systematic effect related to the effective curvature of the pentaprism, which is coupled to the tilt angle of the SUT and its distance from the pentaprism. The character of this systematic effect is determined through the following analysis.

A ray exiting the autocollimator in the  $\hat{x}$  direction towards a curved mirror (model of the pentaprism) is incident at point  $P_1$ , which has coordinates  $(x_1, y_1)$ . The normal vector  $\hat{n}_1$  at  $P_1$  points in the direction  $(\cos \phi, -\sin \phi)$ , where  $\phi = \pi/4$ . For simplicity we assume the curved mirror has a cylindrical shape. We use a coordinate system that has its origin at the center of the cylindrical mirror. The surface under test is located at point  $P_2$  with coordinates  $(x_1, y_1 - d)$ , where  $d$  is the distance to surface under test. The angle of the ray reflected from the SUT will be equal to twice its tilt angle  $V$ , which is the quantity of interest measured by the autocollimator. This ray will be incident upon the cylindrical mirror at a point  $P_3$  with a normal vector  $\hat{n}_3$ . The angle between  $\hat{n}_1$  and  $\hat{n}_3$  is precisely the error introduced by the curvature of the reflecting surface. Thus, determining the error is reduced to solving for the coordinates of  $P_3$ , from which it is straightforward to determine the normal vector.

Using the definitions for  $w$  and  $h$  as shown in Fig. 1, the coordinates for  $P_3$  can be written as  $(x_1 - w, y_1 - d + h)$ . Then, from the geometry of the problem we can extract a pair of equations that determine  $w$  and  $h$ ,

$$\tan V = \frac{w}{h}; \quad (1)$$

$$(x_1 - w)^2 + (y_1 - d + h)^2 - R^2 = 0, \quad (2)$$

where  $R$  is the radius of the cylindrical mirror, which models the curvature of the pentaprism. If we define

$$\beta \equiv \arctan\left(\frac{y_1 - d + h}{x_1 - w}\right) \quad (3)$$

Then the normal vector  $\hat{n}_3$  is given by

$$\hat{n}_3 = [\cos \beta, -\sin \beta] \quad (4)$$

From this equation it is possible to determine the error in the measured  $V$  angle as a function of the distance to the SUT  $d$  and the effective radius of curvature of the pentaprism  $R$ .

At this point, it is useful to examine a specific case, namely the DLTP.<sup>10,11</sup> In its original form,<sup>11</sup> a bulk pentaprism with an aperture size of 30 mm  $\times$  30 mm was used. In order to minimize the systematic error, five pentaprisms made of Homosil 101 were fabricated with the specified surface quality of  $\lambda/10$ , s/d 40/20, angle tolerance 3", and with anti-reflection coating on the two working surfaces. The pentaprisms were carefully tested with the ZYGO<sup>TM</sup> GPI interferometer and the best pentaprism, which had an effective radius of curvature of about 350 m,<sup>11</sup> was selected for the DLTP. The effective radii of curvature for the remaining four pentaprisms were on the order of 200 m. In typical operation, the SUT is placed 0.14 m from the center of the pentaprism.

Using the above numbers for  $d$  and  $R$ , we can estimate the systematic effect incurred in measurements of a curved optic. Figure 2 shows a plot of the error in the measured angle  $V$  in  $\mu$ rad versus the actual tilt angle  $V$  of the SUT in mrad. The error is determined as the difference in the actual tilt angle  $V$  of the SUT and the measured (simulated) autocollimator reading of the angle  $V$  in the vertical direction.<sup>10</sup> The range of the horizontal axis in Fig. 2, is chosen to correspond to the measurable range of the autocollimator used in the DLTP.<sup>11</sup> We can interpret this data as a linear error term of 1.1  $\mu$ rad/mrad. The existence of this type of error will affect the determination of the figure and can also result in an increased rms slope variation. As an

example, consider an ideal 15.000 m spherical optic. The measured radius would be 14.983 m with an rms slope variation of 0.018  $\mu\text{rad}$ . The non zero rms slope variation appears because the error due to the effective curvature is not entirely linear, even in the simplified case of a cylindrical curvature.

The effective curvature of the MBPP currently in use on the DLTP has been measured to be 9000 m.<sup>10</sup> In this case, the systematic error is reduced by a factor of 25, thus contributing a linear error term of only 0.04  $\mu\text{rad/mrad}$ . Using the same example of the ideal 15.000 m spherical mirror, the measured radius of curvature would be 14.999 m with an rms slope variation of 0.001  $\mu\text{rad}$ .

Recall that preceding analysis was performed assuming the effective curvature of the pentaprism took a cylindrical shape. In reality, the effective shape of the pentaprism will be more complex, but the same the basic results as above will apply.

It is also worthwhile to mention the cost benefits. A single bulk pentaprism, like that which is mentioned above, costs on the order of \$1,000, whereas the mirrors used for the MBPP cost on the order of \$100. Thus, together with kinematic mounts, the MBPP, basically speaking, offers the same cost at about 25 times increase in performance.

### **3. ALIGNMENT PROCEDURES**

#### **3.1 Background**

The primary concern when using an MBPP is the ability to achieve optimal alignment. Traditional bulk pentaprisms can be fabricated with angular tolerances down to just a few  $\mu\text{rads}$ . A comprehensive study on the alignment of such pentaprisms in deflectometric scanning devices has yielded novel alignment procedure that reduces systematic errors to a sub nrad level.<sup>12</sup> With an MBPP, however, the initial alignment of the two reflecting faces will, in general, be much



worse than that of a precision machined bulk pentaprism. Achieving a high accuracy in the relative orientation of the two mirrors in an MBPP is the focus of this section.

The majority of the terminology and strategy for developing the following procedures is based on Ref.<sup>12</sup> Fundamentally, the present work can be viewed as an extension of the approach described in this work. Although the present work is self consistent, it is suggested that the reader be familiar Ref.<sup>12</sup>

To discuss the alignment of an MBPP we introduce the terms parallel error, denoted by  $\omega$ , and wedge error, denoted by  $\delta$ , Fig. 3a. The wedge error is easily visualized and understood; it's the deviation from the ideal wedge angle of  $45^\circ$  between mirrors M1 and M2 that produces the desired  $90^\circ$  deflection of the incoming beam. The parallel error is the difference in the roll angles of the M1 and M2 mirrors. Sufficiently minimizing the wedge error is straightforward and can be accomplished in a number of ways.<sup>10</sup> Minimizing the parallel error, however, is more complex and requires a dedicated procedure. Note that the slightly different definitions of the two errors in Fig. 3b are made simply to facilitate two different alignment procedures considered below.

Assuming the two mirrors of the MBPP are mounted to adjustable kinematic stages we present two procedures, relevant for different MBPP designs, for minimizing alignment errors. Furthermore, we discuss the influences of residual misalignments on typical measurements within a scanning deflectometric device. For each of these alignment procedures we will assume the MBPP is integrated into a scanning deflectometric device – Fig. 4. Thus, it is assumed that an autocollimator projects a beam that is deflected 90 degrees by the MBPP to probe a surface under test. The vertical and horizontal angles of the returning beam are measured by the

autocollimator. For the purposes of developing an alignment procedure we assume the SUT is an ideally flat surface.

Before delving into the analytical description of the problem, it is prudent to clarify some of the terminology as there are many components and angles involved. The symbols  $\alpha$ ,  $\beta$  and  $\gamma$  will be used to denote pitch, roll and yaw angles with subscripts used to denote the specific component – Fig. 4. With respect to the mirrors M1 and M2, the pitch and roll axes are defined as a pair of orthogonal axes tangential to the mirror’s reflecting face with the origin at the center of the mirror. In the optimal configuration, the pitch axis is parallel to the y axis. The yaw axis would be the axis normal to the mirror’s surface, but rotations about these axes are superfluous.

When rotations of the whole pentaprism are discussed, the pitch, roll and yaw axes are taken to be in the direction of the y, x and z directions, respectively. The origin of this coordinate frame is taken to be the center of the MBPP.

Finally, the axes of rotation for the SUT (Fig. 4) will be similar to those of the M1 and M2 mirrors, i.e. a pair of orthogonal axes which are tangential to the SUT’s surface with the pitch axis parallel to the y axis and the origin at the center of the SUT.

### **3.2 Alignment procedure 1**

The first alignment procedure is relevant for an MBPP design which allows for independent rotations of one of the mirrors M1 and M2 in pitch and roll and rotations of the two mirrors as a whole unit. In this case we use the definitions of parallel error and wedge error as illustrated in Fig. 3a. This type of design is intended to allow the user to align the two mirrors into an optimal optical square arrangement and then independently align the entire unit in a deflectometric scanning device according to the procedure described in Ref.<sup>12</sup> Such a design is particularly useful if it is desired to use the MBPP outside of operations in the deflectometric

scanning device. Once the alignment of the mirrors M1 and M2 relative to each other is achieved, there is no need to adjust them any further. All other alignments can be performed by adjusting the whole unit. Thus, it is simple to adapt the MBPP for other applications. This style of MBPP is currently in use on the DLTP<sup>10,11</sup> at the ALS OML.

Using the same approach as described in Ref.,<sup>12</sup> ray tracing and a correlation analysis produce the following approximations for the measured (simulated) autocollimator readings  $V$  (up to 2<sup>nd</sup> order effects) and  $H$  (up to 1<sup>st</sup> order effects):

$$V \approx -\alpha_{pp}^2 + \alpha_{st}(\alpha_{pp} + \gamma_{pp}) + 2\delta + 2\left\{\sqrt{2}\cos\left(\frac{\pi}{8}\right) \cdot \alpha_{pp} - \sin\left(\frac{\pi}{8}\right) \cdot \alpha_{st}\right\}\omega - \frac{\omega^2}{\sqrt{2}} - \beta_{st}; \quad (5)$$

$$H \approx \alpha_{st} - \alpha_{pp} + \gamma_{pp} + 2\cos\left(\frac{\pi}{8}\right)\omega. \quad (6)$$

The reference coordinate system is set by the autocollimator with  $\alpha_{as} = \beta_{ac} = \gamma_{ac} = 0$ . Therefore, the autocollimator readout is defined as  $\frac{1}{2}$  of the deflection angle of the reflected beam, corresponding to the equivalent tilt angle of the SUT. The subscripts  $pp$ ,  $st$ , and  $ac$  stand for pentaprism, surface under test (Fig. 4), and autocollimator, respectively.

We introduce here the *yaw test* and *roll test*. These are the terms given to two unique procedures which provide two parameters used to guide the optimal angular alignment of the pentaprism and of the surface under test (SUT) relative to the coordinate system of the autocollimator which is provided by its two perpendicular measuring axes and its optical axis. The first term, yaw test, refers to a series of measurements made in order to guide the optimal alignment of a reference flat SUT and autocollimator in relative roll angle. It is accomplished by adjusting the pentaprism about its yaw axis through a range of angles (about  $\pm 4.8$  mrad, this range of angles is chosen to match the measurement range of the autocollimator) and plotting the measured  $V$  (vertical angle) vs.  $H$  (horizontal angle) dependence. There is a linear relation

between these two quantities and when the slope,  $M_{\text{yaw}}$ , is minimized, the relative roll angle between the SUT and autocollimator is also minimized. The second term, roll test, refers to series of measurements made in order to guide the optimal alignment of the pentaprism about its yaw axis. It is performed by adjusting the pentaprism about its roll axis and plotting the  $V$  vs.  $H$  dependence. There is a quadratic relation between these two quantities and the location of the vertex,  $H_{\text{roll}}$ , guides the alignment of the pentaprism about its yaw axis. The pentaprism is optimally aligned in yaw when  $H_{\text{roll}} = 0$ .

The introduction of  $\delta$  and  $\omega$  results in slight modifications in the equations found in Ref.<sup>12</sup> for the parameters  $M_{\text{yaw}}$  and  $H_{\text{roll}}$ :

$$M_{\text{yaw}} = \frac{\partial V}{\partial H} = \frac{\partial V}{\partial \gamma_{\text{pp}}} \left( \frac{\partial H}{\partial \gamma_{\text{pp}}} \right)^{-1} = \alpha_{\text{st}}; \quad (7)$$

$$H_{\text{roll}} = \gamma_{\text{pp}} + \frac{M_{\text{yaw}}}{2} + (2 - \sqrt{2}) \cos\left(\frac{\pi}{8}\right) \omega. \quad (8)$$

Assuming  $M_{\text{yaw}} = 0$  and considering the parabolic dependence of the angle  $V$  on the angle  $H$  during the roll test, its vertex value  $V_{\text{roll}} = V(H_{\text{roll}})$  can be derived from Eqs. (5) - (8) as:

$$V_{\text{roll}} = V(H = H_{\text{roll}}, M_{\text{yaw}} = 0) = 2\delta - \beta_{\text{st}} + \left\{ 2 \cos^2\left(\frac{\pi}{8}\right) - \frac{1}{\sqrt{2}} \right\} \omega^2. \quad (9)$$

Differentiation leads to

$$\frac{\partial V_{\text{roll}}}{\partial \omega} = 2 \left\{ 2 \cos^2\left(\frac{\pi}{8}\right) - \frac{1}{\sqrt{2}} \right\} \omega \quad (10)$$

and therefore

$$\omega = 0 \text{ for } \frac{\partial V_{\text{roll}}}{\partial \omega} = 0. \quad (11)$$

This provides an analytic foundation for the development of an alignment procedure. Experimentally, the above considerations can be realized by performing a series of roll tests in which the roll angle of the M2 mirror  $\omega$  (Fig. 3a) is successively incremented. That is, a roll test is performed, then M2 is adjusted in  $\omega$  and the roll test is repeated, thus yielding a series of quadratic dependences. The vertices of these quadratic dependences themselves exhibit a quadratic dependence, as dictated by (9). The vertex of this quadratic dependence occurs when the parallel error,  $\omega$ , is equal to zero. With the parallel error equal to zero, the value of  $H_{\text{roll}}$  is then used to align the pentaprism unit about its yaw axis.

A note on the accuracy of the approximations in (5) and (6): for a variation of all parameters within  $\pm 480 \mu\text{rad}$ , the  $V$  angle according to (5) deviates no more than 8.1 mrad, and the  $H$  angle according to (6) no more than 1.3  $\mu\text{rad}$  from the exact values derived by ray tracing.

### 3.3 Alignment procedure 2

A second alignment procedure is provided here for an MBPP design, which allows only independent rotations of the mirrors M1 and M2. There is no possibility to manipulate the MBPP as whole unit. The advantage of this design compared to the previous design is that there is one less moving part. Such a design has been implemented in (HZB)/BESSY-II NOM.<sup>5,6</sup>

To facilitate the description of this procedure some new terms are introduced. An M1 or M2 scan refers to a test, similar to the traditional roll test, in which the M1 or M2 mirror is rotated about its roll axis through a range of angles (about  $\pm 4.8$  mrad). The quadratic dependences of the measured (simulated)  $V$  vs.  $H$  values produce two parameters used for guiding alignment,  $H_1$  and  $V_1$  for an M1 scan and  $H_2$  and  $V_2$  for an M2 scan. These parameters represent the locations of the vertices of the quadratic dependences in both the  $H$  and  $V$  angles. A SUT roll test consists of adjusting the SUT about its roll axis through a range of angles (about

$\pm 4.8$  mrad). There is a linear relation between the measured (simulated)  $V$  vs.  $H$  dependence with a slope  $M_{st}$ .

Again, an alignment procedure is developed through the same approach as in Ref.<sup>10</sup> using ray tracing and a correlation analysis. A slight modification of the definition of the parallel and wedge errors have been introduced to account for the independent rotations of M1 and M2,

Fig. 3b. In this case, the  $V$  and  $H$  angles can be rewritten as

$$V \approx \frac{(\omega_1^2 - \omega_2^2)}{\sqrt{2}} + 2 \sin\left(\frac{\pi}{8}\right)(\omega_1 + \omega_2) \alpha_{st} - \sqrt{2} \cdot \omega_1 \omega_2 + 2(\delta_1 + \delta_2) - \beta_{st}; \quad (12)$$

$$H \approx \alpha_{st} + 2 \cos\left(\frac{\pi}{8}\right)(\omega_1 - \omega_2). \quad (13)$$

The M1 scan is described analytically as a variation of  $\omega_1$  with the vertex described by the relation

$$\frac{\partial V}{\partial H} = \frac{\partial V}{\partial \omega_1} \left( \frac{\partial H}{\partial \omega_1} \right)^{-1} = 0. \quad (14)$$

From (12) and (13) we can derive the horizontal angle  $H_1$  of the vertex as

$$H_1 \equiv 0, \quad (15)$$

i.e., its location is zero, independent of the other parameters.

From (14), with the help of (12) and (13), the corresponding vertical angle  $V_1$  of the vertex can be derived as

$$V_1 = V(H_1) = 2(\delta_1 + \delta_2) - \beta_{st} + \frac{(\omega_1 - \omega_2)^2}{\sqrt{2}} - \sqrt{2} \cdot \omega_1^2. \quad (16)$$

Now, a variation of the parallel error  $\omega_2$  of M2 of the optical square is performed.  $V(H)$  can be described by a parabolic function again with its vertex defined by the relation

$$\frac{\partial V}{\partial H} = \frac{\partial V}{\partial \omega_2} \left( \frac{\partial H}{\partial \omega_2} \right)^{-1} = 0. \quad (17)$$

From (12) and (13) we can derive the horizontal angle  $H_2$  of the vertex as

$$H_2 = \frac{\sqrt{2}}{\sin\left(\frac{\pi}{8}\right)} \omega_1. \quad (18)$$

From (17), with the help of (12) and (13), the corresponding vertical angle  $V_2$  of the vertex can be derived as

$$V_2 = V(H_2) = 2(\delta_1 + \delta_2) - \beta_{st} + \frac{(\omega_1 + \omega_2)^2}{\sqrt{2}} + \sqrt{2} \cdot \omega_1^2. \quad (19)$$

From (16) and (19) we can deduce

$$V_1 - V_2 = -2\sqrt{2} \cdot \omega_1(\omega_1 + \omega_2). \quad (20)$$

For completeness, we perform an SUT roll test by a variation of  $\alpha_{st}$ . In this case,  $V(H)$  can be described by a linear function with its slope  $M_{st}$  defined by the relation

$$M_{st} = \frac{\partial V}{\partial H} = \frac{\partial V}{\partial \alpha_{st}} \left( \frac{\partial H}{\partial \alpha_{st}} \right)^{-1} = 2 \sin\left(\frac{\pi}{8}\right) (\omega_1 + \omega_2). \quad (21)$$

The preceding analytic solution provides the framework for understanding the following alignment procedure. The M2 scan is repeated as M1 is incrementally adjusted about its roll axis, with the goal to obtain  $H_2 = 0$ . From (18) it can be seen that an M2 scan that results in  $H_2 = 0$  leads to the conclusion that  $\omega_1 = 0$ . With  $H_2 = 0$  the SUT roll test is repeated while M2 is adjusted about its roll axis until  $M_{st} = 0$ . With  $\omega_1 = 0$ , (21) is simplified to

$$M_{st} = 2 \sin\left(\frac{\pi}{8}\right) (\omega_2), \quad (22)$$

from which it clearly follows that  $\omega_2 = 0$  when  $M_{st} = 0$ . Therefore,  $H_1 = H_2 = 0$  and  $M_{st} = 0$  results in the optimal angular adjustment of the optical square with  $\omega_1 = \omega_2 = 0$ . In this configuration, the MBPP is optimally aligned relative to the autocollimator with the parallel error equal to zero.

### 3.4 Effects of non zero parallel error

Below we perform an analysis on the influences of a non zero parallel error on the performance of slope measurements, including the effect of crosstalk between the tangential and sagittal slopes of the SUT.

Assuming an initial optimal angular adjustment of the SUT and of the optical square according to the procedures described in Ref.<sup>12</sup> and above, i.e.,  $M_{yaw} = 0$ ,  $H_{roll} = 0$ ,  $V_{roll} = 0$ , and  $H = 0$  is initially achieved, then

$$\tilde{\alpha}_{st} = 0, \quad (23)$$

$$\tilde{\beta}_{st} = 2\delta + \left\{ 2 \cos^2\left(\frac{\pi}{8}\right) - \frac{1}{\sqrt{2}} \right\} \omega^2, \quad (24)$$

$$\tilde{\alpha}_{pp} = \sqrt{2} \cos\left(\frac{\pi}{8}\right) \omega, \text{ and} \quad (25)$$

$$\tilde{\gamma}_{pp} = -(2 - \sqrt{2}) \cos\left(\frac{\pi}{8}\right) \omega. \quad (26)$$

Note that  $\gamma_{st}$  (the yaw angle of the SUT, Fig. 4) and  $\beta_{pp}$  (the pitch angle of the optical square) do not need to be considered as they do not influence the measured angles  $V$  and  $H$  according to (5) and (6).

During the measurement of the SUT, a wobble of the pentaprism will introduce additional errors in its angular orientation in roll,  $\Delta\alpha_{pp}$ , and yaw,  $\Delta\gamma_{pp}$ . Furthermore, a change in the sagittal slope of the SUT,  $\Delta\alpha_{st}$ , and in its slope,  $\Delta\beta_{st}$ , are assumed to be present. Therefore,



with (23)-(26), the sagittal slope of the SUT,  $\alpha_{st}$ , its slope,  $\beta_{st}$ , the roll angle of the optical square,  $\alpha_{pp}$ , and its yaw angle,  $\gamma_{pp}$ , are defined as

$$\alpha_{st} = \tilde{\alpha}_{st} + \Delta\alpha_{st} = \Delta\alpha_{st}, \quad (27)$$

$$\beta_{st} = \tilde{\beta}_{st} + \Delta\beta_{st} = 2\delta + \left\{ 2\cos^2\left(\frac{\pi}{8}\right) - \frac{1}{\sqrt{2}} \right\} \omega^2 + \Delta\beta_{st}, \quad (28)$$

$$\alpha_{pp} = \tilde{\alpha}_{pp} + \Delta\alpha_{pp} = \sqrt{2}\cos\left(\frac{\pi}{8}\right)\omega + \Delta\alpha_{pp}, \text{ and} \quad (29)$$

$$\gamma_{pp} = \tilde{\gamma}_{pp} + \Delta\gamma_{pp} = -(2 - \sqrt{2})\cos\left(\frac{\pi}{8}\right)\omega + \Delta\gamma_{pp}. \quad (30)$$

Putting (27)-(30) in (5) results in the measured  $V$  angle

$$V = \Delta\alpha_{st}(\Delta\alpha_{pp} + \Delta\gamma_{pp}) - (\Delta\alpha_{pp})^2 - \Delta\beta_{st}. \quad (31)$$

Therefore, the error  $\Delta V$  in the measurement of changes in the slope of the SUT,  $\Delta\beta_{st}$ , is given by

$$\Delta V = \Delta\alpha_{st}(\Delta\alpha_{pp} + \Delta\gamma_{pp}) - (\Delta\alpha_{pp})^2. \quad (32)$$

Equation (32) leads to several important conclusions. Firstly, as long as an initial optimal angular adjustment of the SUT and of the optical square is performed, the wedge error  $\delta$  and the parallel error  $\omega$  are irrelevant to the measurement of the SUT's tangential slope. This reduces the burden on the adjustment of the reflecting faces of the optical square. The approximations from (5) and (6) are accurate to better than 9 nrad for variation of all parameters within +/- 0.5 mrad. Accordingly, minimizing the wedge and parallel errors to the level of 0.5 mrad and applying the optimal alignment procedure eliminates all systematic errors due to the misalignments present in the optical square to below 9 nrad, well below the typical noise level of an autocollimator.

Secondly, in the presence of angular errors  $(\Delta\alpha_{pp} + \Delta\gamma_{pp}) \neq 0$  in the roll and yaw orientation of the optical square during its movement, changes in the sagittal slope of the SUT,  $\Delta\alpha_{st}$ , result in residual  $V$  angle errors (due to the mutual interaction of the angular errors, i.e. crosstalk) which affect the measurement of the SUT's tangential slope. However, these contributions are of second order in angle.

For completeness: putting (27)-(30) in (6) results in the measured  $H$  angle

$$H = \Delta\alpha_{st} + \Delta\gamma_{pp} - \Delta\alpha_{pp}. \quad (33)$$

Therefore, the error  $\Delta H$  in the measurement of changes in the sagittal slope of the SUT,  $\Delta\alpha_{st}$ , is given by

$$\Delta H = \Delta\gamma_{pp} - \Delta\alpha_{pp}. \quad (34)$$

Again, note that the optimal alignment procedure renders the wedge and parallel errors irrelevant, as is the case for the measured  $V$  angle. However, with the  $H$  angle the error contributions from changes in angular orientation of the optical square, i.e. due to wobble, contribute in the first order. Consequently, an optical square (or pentaprism) achieves no error reduction with respect to measurement of the sagittal slope of the SUT.

#### 4. CONCLUSION

We have analytically examined the opportunity to improve the performance of typical optical scanning deflectometric instruments through the use of a mirror based pentaprism instead of traditional bulk material pentaprisms. The motivation for this switch is to remove any potential complexities due to the homogeneity of the bulk material and to improve upon the effective curvature. We have provided an analysis of the errors introduced to slope measurements as a result of this curvature. It has been shown that this type of error affects the

overall determination of the figure of an optic and can lead to an increase in the measured rms slope variation due to its non linear character.

As has been shown in Ref.<sup>10</sup>, an MBPP can be assembled using relatively inexpensive gold coated mirrors such that the effective curvature is reduced by a factor of 25 compared to a far more expensive precision machined bulk pentaprism. As the systematic error depends on the effective radius of curvature of the pentaprism to first order, an MBPP will suppress this spurious effect by a factor of 25.

The advantages of precision machined pentaprisms lie in the tight tolerances on angular errors of the relative orientation of the reflecting and refracting faces as well as their stability. However, through a comprehensive analytical review of two different MBPP designs we have determined the following. Easily executable alignment methods exist and have been suggested. Residual misalignments of the MBPP on the order of 0.5 mrad contribute entirely negligible errors to slope measurements.

The two MBPP designs reviewed have specific advantages. The design which allows global rotation of the MBPP (rotations of the entire MBPP unit) allows one to follow the robust alignment procedure described in Ref.<sup>12</sup> after properly aligning the M1 and M2 mirrors. It also allows for easy integration of the MBPP into other applications. The second design in which the independent rotations of M1 and M2 are the only degrees of freedom will have improved stability compared with the previous design as there is one less moving part.

Finally, the experimental results provided in Ref.<sup>10</sup> are in excellent agreement with the analytic considerations provided here.

## **ACKNOWLEDGEMENTS**

The Advanced Light Source is supported by the Director, Office of Science, Office of Basic Energy Sciences, Material Science Division, of the U.S. Department of Energy under Contract No. DE-AC02-05CH11231 at Lawrence Berkeley National Laboratory.

## **DISCLAIMER**

This document was prepared as an account of work sponsored by the United States Government. While this document is believed to contain correct information, neither the United States Government nor any agency thereof, nor The Regents of the University of California, nor any of their employees, makes any warranty, express or implied, or assumes any legal responsibility for the accuracy, completeness, or usefulness of any information, apparatus, product, or process disclosed, or represents that its use would not infringe privately owned rights. Reference herein to any specific commercial product, process, or service by its trade name, trademark, manufacturer, or otherwise, does not necessarily constitute or imply its endorsement, recommendation, or favoring by the United States Government or any agency thereof, or The Regents of the University of California. The views and opinions of authors expressed herein do not necessarily state or reflect those of the United States Government or any agency thereof or The Regents of the University of California.

## References

1. L. Assoufid, O. Hignette, M. Howells, S. Irick, H. Lammert, and P. Takacs, "Future metrology needs for synchrotron radiation grazing-incidence optics," *Nucl. Instr. and Meth. A* **467-468**, 267-70 (2001).
2. P. Z. Takacs, "X-ray optics metrology," in M. Bass (Ed.), *Handbook of Optics*, third ed., vol. V, chapter 46, McGraw-Hill Publishing Company, New York (2009).
3. E. Debler, K. Zander, Ebenheitsmessung an optischen Planflächen mit Autokollimationsfernrohr und Pentagonprisma, PTB Mitteilungen Forschen + Prüfen, Amts und Mitteilungsblatt der Physikalisch Technischen Bundesanstalt, Braunschweig und Berlin, 339-349 (1979).
4. F. Siewert, T. Noll, T. Schlegel, T. Zeschke, and H. Lammert, "The Nanometer Optical Component Measuring machine: a new Sub-nm Topography Measuring Device for X-ray Optics at BESSY," *AIP Conference Proceedings* **705**, 847-850 (2004).
5. H. Lammert, T. Noll, T. Schlegel, F. Siewert, and T. Zeschke, Optisches Messverfahren und Präzisionsmessmaschine zur Ermittlung von Idealformabweichungen technisch polierter Oberflächen, Patent No.: DE 103 03 659 (28 July 2005).
6. F. Siewert, H. Lammert, and T. Zeschke, "The Nanometer Optical Component Measuring Machine," *Modern Developments in X-ray and Neutron Optics*, Springer-Verlag, Berlin/Heidelberg, (2008).
7. R. D. Geckeler, and I. Weingärtner, "Sub-nm topography measurement by deflectometry: flatness standard and wafer nanotopography," *Proc. SPIE*, **4779**, 1-12 (2002).
8. J. Illema, and M. Wurm, "Deflectometric Measurements of Synchrotron-Optics for Postprocessing," *AIP Conference Proceedings* **705**, 843-846 (2004).

9. R. D. Geckeler, "ESAD Shearing Deflectometry: Potentials for Synchrotron Beamline Metrology," *Proc. SPIE* **6317**, 1–12 (2006).
10. S. K. Barber, G. Y. Morrison, V. V. Yashchuk, M. V. Gubarev, R. D. Geckeler, J. Buchheim, F. Siewert, and T. Zeschke, "Developmental long trace profiler using optimally aligned mirror based pentaprism," *Proc. SPIE* **7801**, 7801-2/1-12 (2010); *Opt. Eng.* **50**(5) (2011), in press.
11. V. V. Yashchuk, S. K. Barber, E. E. Domning, J. L. Kirschman, G. Y. Morrison, B. V. Smith, F. Siewert, T. Zeschke, R. D. Geckeler, and A. Just, "Sub-microradian Surface Slope Metrology with the ALS Developmental Long Trace Profiler," *Nucl. Instr. and Meth. A* **616**, 212-223 (2010).
12. R. D. Geckeler, "Optimal use of pentaprisms in highly accurate deflectometric scanning," *Meas. Sci. Technol.* **18**, 115-125 (2007).
13. Shinan Qian, Werner Jark, Peter Z. Takacs, "The penta-prism LTP: A long-trace-profiler with stationary optical head and moving penta prism," *Rev. Sci. Instrum.* **66**(3), 2562-2569(1995).

## **Biographies**

**Samuel K. Barber** received his BS degree in physics University of California at Los Angeles in 2007. He joined the Optical Metrology Laboratory at the Advanced Light Source, Lawrence Berkeley National Laboratory in 2008 where he worked on x-ray optical instrumentation and metrology. Currently he is pursuing a PhD in physics at the University of California at Los Angeles.

**Ralf D. Geckeler** received his PhD from the Eberhard-Karls University, Tübingen, Germany, in 1998. He heads the ‘Angle Metrology’ Group at the ‘Precision Engineering’ Division of the Physikalisch-Technische Bundesanstalt (PTB), Braunschweig, the National Metrology Institute of Germany. The group focuses on research and development, as well as calibration, of angle measuring devices, such as autocollimators and angle encoders, in international collaboration with industry and research institutes. Current research topics include the improvement of autocollimator performance and calibration, especially at small beam diameters, the advancement of angle metrology for the characterization of beamline optics at synchrotron facilities worldwide, and the development of methods and advanced mathematical algorithms for angle encoder calibration.

**Valeriy V. Yashchuk** received his MS degree in experimental physics from St. Petersburg State University (Russia) in 1979, and his PhD degree from St. Petersburg Nuclear Physics Institute (Russia) in 1994. He is currently leading the Optical Metrology Laboratory at the Advanced Light Source, Lawrence Berkeley National Laboratory. He has authored more than 60 scientific articles in the fields of atomic and molecular physics, nonlinear optics, electro- and magneto-optics, laser spectroscopy, experimental scientific methods and instrumentation, and optical metrology. In 1986 for the development of a method of reduction of phase space of an

atomic beam he was awarded the Leningrad Komsomol Prize in physics. In 2007, he received R&D Magazine's R&D 100 Award for development of Laser-Detected MRI. His current research interest is in x-ray optics, optical instrumentation and metrology for x-ray optics.

**Mikhail V. Gubarev** received his MS from the Moscow Physics Engineering Institute in 1988 and his Ph.D. in physics from the University at Albany in 1998. Since 1998 he has been working in the field of x-ray instrumentation, particularly in the development of x-ray and neutron optics, optical metrology methods, x-ray detectors, at the Marshall Space Flight Center. In recent years he has focused on high angular resolution hard-x-ray optics for astrophysical applications.

**Jana Buchheim** received her BA in Engineering from the Berlin School of Economics and Law (Germany) in 2008. Since 2008 she is working as research engineer at the BESSY-II Optical Systems Group of the Helmholtz-Zentrum Berlin. She is mainly working on improving of optical metrology instrumentation and characterizing state of the art X-ray optical systems at the BESSY-II Optics Laboratory.

**Frank Siewert** received his Dipl.-Ing. (TU) in Metallurgy and Material Sciences from the Technical University Bergakademie Freiberg (Germany) in 1989. From 1989 – 1991 he was working on the field of Powder Metallurgy at the BMHW in Berlin. He then joined the DLR-Institute for Space Sensor Systems in Berlin working on the CASSINI - Cosmic Dust Analyzer from 1991 - 1995. From 1996 – 2000 he was with O&K Optikkomponenten & Kristalle developing finishing technology for crystal-materials. Since 2000 he is staff scientist at the BESSY-II Optical Systems Group of the Helmholtz-Zentrum Berlin. He currently is responsible for the BESSY-II Optics Laboratory. For his contribution to the development of the Nanometre Optical Component Measuring Machine (NOM) he received the European Innovation Award on



Synchrotron Radiation 2009. His current research interest is in X-ray optics, SR-Instrumentation and metrology.

**Thomas Zeschke** received his Diplom-Ingenieur (academically qualified engineer) in Precision Engineering from the Friedrich-Schiller-University Jena in 1989. From 1989 - 1993 he worked at the engineering department of a chromatograph manufacturer in Berlin. Since 1993 he is R&D engineer at the BESSY-II Optical Systems Group of the Helmholtz-Zentrum Berlin. In 2009 he received together with his colleagues an Innovation-Award on Synchrotron Radiation for the development of an ultraprecise measuring machine for optical surfaces (Nanometer Optical Component Measuring Machine - NOM). His interests are in the development of technical solutions and methods in the fields of synchrotron beamline instrumentation and metrology for X-ray optics.

**Figures and Figure captions:**

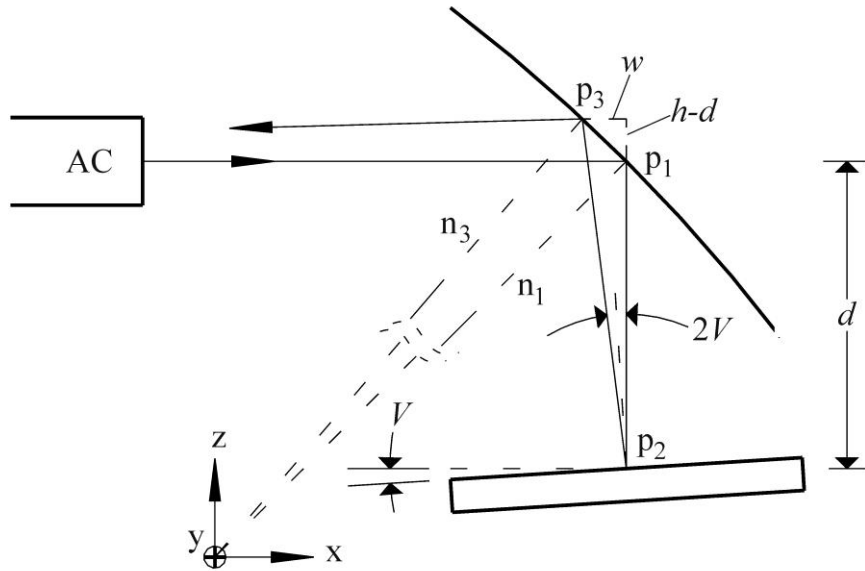


Figure 1: Simplified schematic of scanning deflectometric measurement device with pentaprism modeled as spherical mirror to account for the effective curvature. The angle between  $\hat{n}_1$  and  $\hat{n}_3$  is exactly the systematic error introduced to the measurements. The coordinate system is provided by the autocollimator's optical axis and its two perpendicular measuring axes. The corresponding measuring angles are the vertical angle  $V$  (deflection in  $XZ$ -plane) and the horizontal angle  $H$  (deflection in  $XY$ -plane).

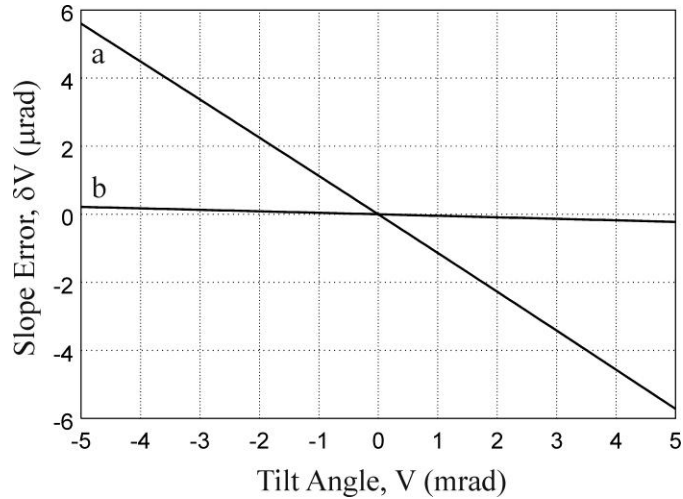


Figure 2: Plot of the error  $\delta V$  in the measured angle  $V$  in  $\mu\text{rad}$  versus the actual tilt angle  $V$  of the SUT in  $\text{mrad}$  for an effective radius of curvature of 350 m (a) and 9000 m (b). The error is determined as the difference in the actual tilt angle  $V$  of the SUT and the measured (simulated) autocollimator reading of the angle  $V$ . The slopes change sign if the curvature is convex instead of concave.

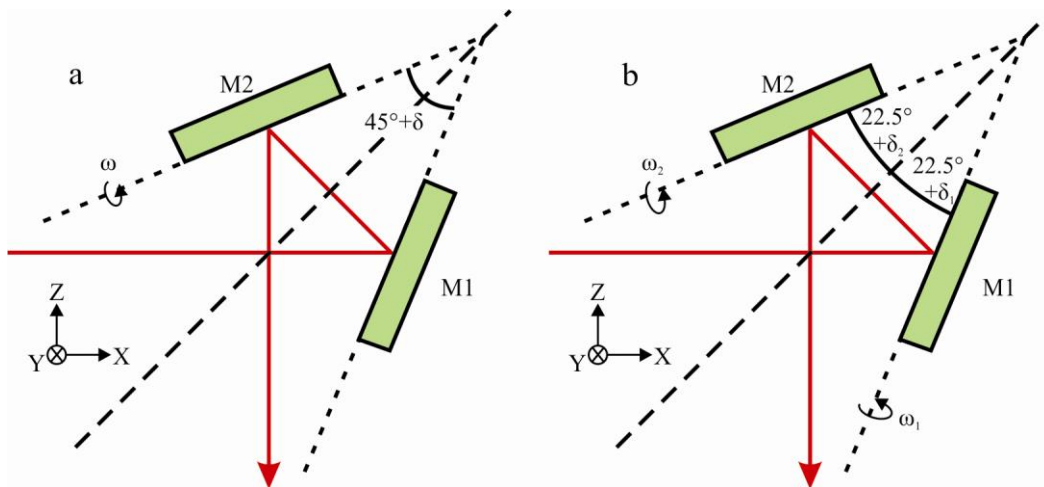


Figure 3: Simplified schematic of mirror based pentaprisms showing the relevant errors. The use of the two different definitions for the errors are made to facilitate the analytic solutions to the development of the optimal alignment procedures for two different MBPP designs.

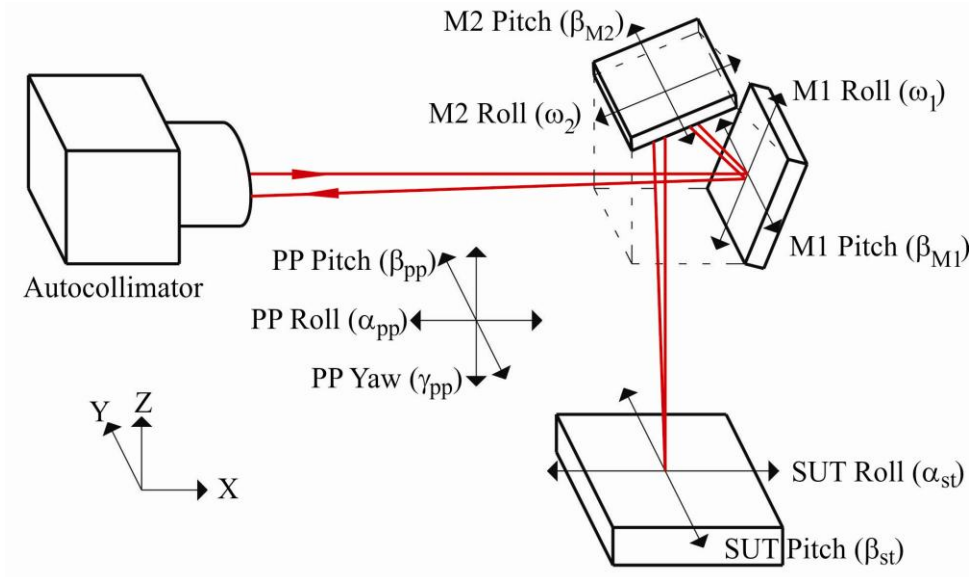


Figure 4: Schematic of scanning deflectometric profiler with mirror based pentaprism. The coordinate systems, relevant to the discussion in the text are shown. M1 and M2 can be rotated about two axes that are M1 and M2 pitch and roll axes. The SUT can be rotated about two axes (SUT pitch and roll axes). The coordinate system for simultaneous rotation of the two mirrors about three axes (PP pitch, roll, and yaw axes) is also shown to facilitate the discussion of the optimal alignment procedures for two different MBPP designs.